Results in Physics 42 (2022) 105964

Contents lists available at ScienceDirect

Results in Physics

journal homepage: www.elsevier.com/locate/rinp

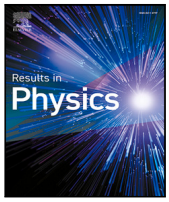

Numerical treatments for the optimal control of two types variable-order COVID-19 model

Nasser Sweilam [a,*], Seham Al-Mekhlafi [b,c], Salma Shatta [d], Dumitru Baleanu [e,f]

[a] Department of Mathematics, Faculty of Science, Cairo University, Giza, Egypt
[b] Department of Mathematics, Faculty of Education, Sana'a University, Yemen
[c] Department of Engineering Mathematics and Physics, Future University in Egypt, Egypt
[d] Department of Mathematics, Faculty of Science, Helwan University, Cairo, Egypt
[e] Cankaya University, Department of Mathematics, Turkey
[f] Institute of Space Sciences, Magurele-Bucharest, Romania

ARTICLE INFO

MSC:
49M25
26A33
65L03

Keywords:
COVID-19 epidemic models
Caputo's derivatives
Optimal control theory
Stability analysis
Non-standard generalized Runge–Kutta methods

ABSTRACT

In this paper, a novel variable-order COVID-19 model with modified parameters is presented. The variable-order fractional derivatives are defined in the Caputo sense. Two types of variable order Caputo definitions are presented here. The basic reproduction number of the model is derived. Properties of the proposed model are studied analytically and numerically. The suggested optimal control model is studied using two numerical methods. These methods are non-standard generalized fourth-order Runge–Kutta method and the non-standard generalized fifth-order Runge–Kutta technique. Furthermore, the stability of the proposed methods are studied. To demonstrate the methodologies' simplicity and effectiveness, numerical test examples and comparisons with real data for Egypt and Italy are shown.

Introduction

Coronaviruses are a large family of viruses that are known to cause illness ranging from the common cold to more severe diseases such as severe acute respiratory syndrome (SARS). The World Health Organization (WHO) has described this variant as a variant of serious concern. The pandemic started in late December 2019 with patients admitted to hospitals with an initial diagnosis of pneumonia in Wuhan, the capital of Hubei, China. In the months that followed, the World Health Organization recorded 1,133,758 total cases and 62,784 fatalities globally in a report dated 5 April 2020. Italy has been severely affected. The first Italy's COVID-19 patient was detected on 21 February 2020 in a little town near Milan, in the northern region of Lombardy, for more details see [1].

Recently, scientific researches focus on the study the coronavirus infection in different scenarios, see for example [2–4].

Also, optimal control theory has successful applications in biological and medical problems. Furthermore, fractional optimal control problems are a subclass of optimal control whose dynamics are described by fractional differential equations. We can minimize the impact of COVID-19 pandemics by minimizing the number of detected asymptomatic infected people who acquire life threatening symptoms and the threatened percentage populations that become extinct. Fractional derivatives are non-local in nature but the integer order derivative can be used to characterize the short memory in time-dependent systems, whereas the variable-order fractional derivative (VOFD) is known for explaining the impacts of long variable memory [5–13] in time-dependent systems. Sweilam et al. recently published several research papers in filed of variable-order optimal control problems (VOCPs), for more details see [14–16].

In this article, we will study numerically the optimal control for two types of variable-order COVID-19 epidemic models. We consider the available data of daily confirmed cases in Italy, from 20 of February 2020 to 5 of April 2020 and in Egypt from 9 March to 13 June, 2020 [17]. The variable-order fractional derivative is defined in the Caputo sense. Two methods will be used to study the suggested model. Non-standard generalized Runge–Kutta of fourth-order method (NGRK4M) and the non-standard generalized Runge–Kutta of fifth-order method

* Corresponding author.
E-mail addresses: nsweilam@sci.cu.edu.eg (N. Sweilam), smdk100@gmail.com (S. Al-Mekhlafi), salmaasaad34@gmail.com (S. Shatta), dumitru@cankaya.edu.tr (D. Baleanu).

https://doi.org/10.1016/j.rinp.2022.105964
Received 16 July 2022; Received in revised form 22 August 2022; Accepted 31 August 2022
Available online 5 September 2022

(NGRK5M) are constructed. Comparative studies between these methods are presented. Comparisons with real data for Egypt and Italy are implemented.

The remainder of this paper is organized as follows: Two types of variable-order fractional and some definitions are given in Section "Basic Notations". In Section "COVID-19 Variable Order Mathematical Model", the COVID-19 model of variable-order with required analysis of equilibrium points is given. Formulation of variable-order optimal control problem is introduced in Section "Formulation of the Control Problem". Two numerical approaches are introduced for solving the suggested model in Section "Numerical Methods". We simulated numerically the proposed model in Section "Numerical Simulations". In Section "Conclusions", the conclusions are presented .

Basic notations

In the following problem:

$$ {}_0^C D_t^{\alpha(t)} y(t) = f(t, y(t)), \quad T \geq t > 0, \quad 1 \geq \alpha(t) > 0, \tag{1} $$

$y(0) = y_o$.

We introduce the Caputo variable-order fractional derivative, where $-\infty < a < b < +\infty$, $\alpha \in \mathbb{C}$, $\Re(\alpha) > 0$, as follows [8]:

Definition 1. The right-left side Caputo's derivatives of order $\alpha(t)$ type one (CVOT1) where $f(t)$ is continuous function are defined respectively as follows [18]:

$$ \begin{aligned} {}_t^C D_b^{\alpha(t)} f(t) &= \frac{1}{\Gamma(n-\alpha(t))} \int_t^b \frac{f^n(s)}{(s-t)^{1+\alpha(t)-n}} ds, \quad t < b, \\ {}_a^C D_t^{\alpha(t)} f(t) &= \frac{1}{\Gamma(n-\alpha(t))} \int_a^t \frac{f^n(s)}{(t-s)^{1-n+\alpha(t)}} ds, \quad a < t. \end{aligned} \tag{2} $$

Definition 2. The right-left side Caputo's derivatives of order $\alpha(t)$ type two (CVOT2), where $f(t)$ is continuous function are defined respectively as follows [18]:

$$ \begin{aligned} {}_t^C D_b^{\alpha(t)} f(t) &= \int_t^b \frac{1}{\Gamma(n-\alpha(s))} \frac{f^n(s)}{(s-t)^{1+\alpha(s)-n}} ds, \quad t < b, \\ {}_a^C D_t^{\alpha(t)} f(t) &= \int_a^t \frac{1}{\Gamma(n-\alpha(s))} \frac{f^n(s)}{(t-s)^{1+\alpha(s)-n}} ds, \quad t > a. \end{aligned} \tag{3} $$

COVID-19 variable order mathematical model

In the following, the COVID-19 model described in [2] will be developed here to variable-order fractional model. The model's variables and the parameters are listed in Tables 1 and 2 respectively. In the following, the updated nonlinear variable-order mathematical model:

$$ {}_0^C D_t^{\alpha(t)} S(t) = -S(t)(\beta^{\alpha(t)} I(t) + \beta_D^{\alpha(t)} I_D(t) + \gamma^{\alpha(t)} I_A(t) + \delta^{\alpha(t)} I_R(t)), \tag{4} $$

$$ \begin{aligned} {}_0^C D_t^{\alpha(t)} I(t) &= S(t)(\beta^{\alpha(t)} I(t) + \beta_D^{\alpha(t)} I_D(t) + \gamma^{\alpha(t)} I_A(t) + \delta^{\alpha(t)} I_R(t)) \\ &\quad - (\varepsilon^{\alpha(t)} + \zeta^{\alpha(t)} + \rho_I^{\alpha(t)}) I(t), \end{aligned} \tag{5} $$

$$ {}_0^C D_t^{\alpha(t)} I_D(t) = \varepsilon^{\alpha(t)} I(t) - (\eta^{\alpha(t)} + \rho_D^{\alpha(t)}) I_D(t), \tag{6} $$

$$ {}_0^C D_t^{\alpha(t)} I_A(t) = \zeta^{\alpha(t)} I(t) - (\varepsilon_A^{\alpha(t)} + \mu^{\alpha(t)} + \kappa^{\alpha(t)}) I_A(t), \tag{7} $$

$$ {}_0^C D_t^{\alpha(t)} I_R(t) = \eta^{\alpha(t)} I_D(t) + \varepsilon_A^{\alpha(t)} I_A(t) - (\nu^{\alpha(t)} + \xi^{\alpha(t)}) I_R(t), \tag{8} $$

$$ {}_0^C D_t^{\alpha(t)} I_T(t) = \mu^{\alpha(t)} I_A(t) + \nu^{\alpha(t)} I_R(t) - (\sigma^{\alpha(t)} + d^{\alpha(t)}) I_T(t), \tag{9} $$

$$ {}_0^C D_t^{\alpha(t)} I_H(t) = \rho_I^{\alpha(t)} I(t) + \rho_D^{\alpha(t)} I_D(t) + \kappa^{\alpha(t)} I_A(t) + \xi^{\alpha(t)} I_R(t) + \sigma^{\alpha(t)} I_T(t), \tag{10} $$

$$ {}_0^C D_t^{\alpha(t)} I_E(t) = d^{\alpha(t)} I_T(t). \tag{11} $$

Let,

$$ I + S + I_D + I_A + R + I_H + I_E I_T = N, $$

Table 1
Variables of the proposed model [2].

Variables	Description
$S(t)$	The susceptible population.
$I(t)$	The infected population with asymptomatic infected and undetected.
$I_D(t)$	The diagnosed population with asymptomatic infected and detected.
$I_A(t)$	The ailing population with symptomatic infected and undetected.
$I_R(t)$	The recognized population with symptomatic infected and detected.
$I_T(t)$	The threatened population which infected with life-threatening symptoms and detected.
$I_H(t)$	The recovered population.
$I_E(t)$	The extinct population.

Table 2
All of the parameters in the proposed model, as well as their meanings [2].

Symbol	Definition	Values
t	Time $t \geq 0$.	
$\beta^{\alpha(t)}$	The transmission rate between a susceptible and an infected population	$(0.57)^{\alpha(t)}$
$\beta_D^{\alpha(t)}$	The transmission rate between a susceptible and diagnosed population.	$(0.0114)^{\alpha(t)}$
$\gamma^{\alpha(t)}$	The transmission rate between a susceptible and ailing population.	$(0.456)^{\alpha(t)}$
$\delta^{\alpha(t)}$	The transmission rate between a susceptible and a recognized population.	$(0.011)^{\alpha(t)}$
$\varepsilon^{\alpha(t)}$	The detection rate, with respect to (w. r. t) relative to asymptomatic cases.	$(0.171)^{\alpha(t)}$
$\varepsilon_A^{\alpha(t)}$	The detection rate w. r. t relative to symptomatic cases.	$(0.3705)^{\alpha(t)}$
$\zeta^{\alpha(t)}$	The rate which infected is not mindful of being infected creates clinically pertinent side effects and is comparable within the nonappearance of a particular treatment.	$(0.1254)^{\alpha(t)}$
$\eta^{\alpha(t)}$	The rate which infected mindful of being infected, creates clinically pertinent indications, and is comparable within the nonappearance of a particular treatment.	$(0.1254)^{\alpha(t)}$
$\mu^{\alpha(t)}$	If there is no known specific medicine that is effective against the illness, the rate at which infected persons are unaware creates life-threatening symptoms.	$(0.0171)^{\alpha(t)}$
$\nu^{\alpha(t)}$	the rate at which infected aware develop life-threatening symptoms; they are comparable if there is no known specific treatment that is effective against the disease.	$(0.0274)^{\alpha(t)}$
$\rho_I^{\alpha(t)}$	The recovered infected population rate.	$(0.0342)^{\alpha(t)}$
$\kappa^{\alpha(t)}$	The recovered ailing population rate.	$(0.0171)^{\alpha(t)}$
$\sigma^{\alpha(t)}$	The recovered threatened population rate.	$(0.017)^{\alpha(t)}$
$\xi^{\alpha(t)}$	The recovered recognized population rate.	$(0.017)^{\alpha(t)}$
$\rho_D^{\alpha(t)}$	The recovered diagnosed population rate.	$(0.0342)^{\alpha(t)}$
$d^{\alpha(t)}$	The death rate.	$(0.01)^{\alpha(t)}$

and N is the total population. The initial conditions are given as follows:

$$ S(0) = S_0, I(0) = I_0, I_D(0) = I_{D0}, I_A(0) = I_{A0}, I_R(0) = I_{R0}, $$
$$ I_T(0) = I_{T0}, I_H(0) = I_{H0}, I_E(0) = I_{E0}. $$

The basic reproduction number

To describe the fundamental of reproductive number (R_o), for more information, see [19]. Consider the matrices F and V where, the matrix F representing the new infection terms and V representing the remaining transfer terms associated with the baseline model are given, respectively, by:

$$V = \frac{\partial G_i}{\partial x_j}, \quad F = \frac{\partial \mathcal{H}_i}{\partial x_j},$$

where G is the individuals transfer rate into or out infected class i from subsystem (6)–(10). The order of infected variables $x_j = (I, I_D, I_A, I_R, I_T)$ and $\alpha(t) \in (0, 1]$ and $\mathcal{H}$ is the appearance rate of new infected individuals in class i,

Then $R_o = \rho(FV^{-1})$, where ρ is the spectral radius of the matrix FV^{-1}. Also,

$$\mathcal{H} = \begin{pmatrix} H_1 \\ H_2 \\ H_3 \\ H_3 \\ H_5 \end{pmatrix} = \begin{pmatrix} S(\beta^{\alpha(t)} I + \beta_D^{\alpha(t)} I_D + \gamma^{\alpha(t)} I_A + \delta^{\alpha(t)} I_R) \\ 0 \\ 0 \\ 0 \end{pmatrix}$$

and

$$G = \begin{pmatrix} G_1 \\ G_2 \\ G_3 \\ G_4 \\ G_5 \end{pmatrix} = \begin{pmatrix} (\varepsilon^{\alpha(t)} + \zeta^{\alpha(t)} + \rho_I^{\alpha(t)}) I \\ (\eta^{\alpha(t)} + \rho_D^{\alpha(t)}) I_D - \varepsilon^{\alpha(t)} I, \\ (\varepsilon_A^{\alpha(t)} + \mu^{\alpha(t)} + \kappa^{\alpha(t)}) I_A - \zeta^{\alpha(t)} I \\ (\nu^{\alpha(t)} + \xi^{\alpha(t)}) I_R - \eta^{\alpha(t)} I_D - \varepsilon_A^{\alpha(t)} I_A \\ \mu^{\alpha(t)} I_A + (\sigma^{\alpha(t)} + d^{\alpha(t)}) I_T - \nu^{\alpha(t)} I_R, \end{pmatrix}.$$

At $E_o = (1, 0, 0, 0, 0, 0, 0, 0)$, where E_o is the disease-free equilibrium point. The basic reproduction number R_0 for the system (4)–(11) is [20]:

$$R_0 = \rho(FV^{-1}) = \frac{\beta^{\alpha(t)}}{r_1} + \frac{\varepsilon^{\alpha(t)} \beta_D^{\alpha(t)}}{r_1 r_2} + \frac{\zeta^{\alpha(t)} \gamma^{\alpha(t)}}{r_1 r_3} + \frac{\delta^{\alpha(t)} (r_2 \zeta^{\alpha(t)} \varepsilon_A^{\alpha(t)} + r_3 \varepsilon^{\alpha(t)} \eta^{\alpha(t)})}{r_1 r_2 r_3 r_4},$$

where $r_1 = \varepsilon^{\alpha(t)} + \zeta^{\alpha(t)} + \rho_I^{\alpha(t)}$, $r_2 = \eta^{\alpha(t)} + \rho_D^{\alpha(t)}$, $r_3 = \varepsilon_A^{\alpha(t)} + \mu^{\alpha(t)} + \kappa^{\alpha(t)}$, $r_4 = \nu^{\alpha(t)} + \xi^{\alpha(t)}$ and $r_5 = \sigma^{\alpha(t)} + d^{\alpha(t)}$.

The effective reproductive number ($R_e(t)$) is the average number of secondary cases of infected population produced in completely susceptible population. The effective reproduction number can be estimated by the product of the basic reproductive number and the susceptible population $S(t)$. So:

$$R_e(t) = S(t) R_0.$$

We have that stability of the system occurs if: $R_e(t) < 1$, and the system becomes unstable if $R_e(t) > 1$.

Equilibrium points

The aim now is to determine the equilibrium points for (4)–(11) and explore their local asymptotic behavior:
${}_0^C D_t^{\alpha(t)} S = {}_0^C D_t^{\alpha(t)} I = {}_0^C D_t^{\alpha(t)} I_D = {}_0^C D_t^{\alpha(t)} I_A = {}_0^C D_t^{\alpha(t)} I_R = {}_0^C D_t^{\alpha(t)} I_T = {}_0^C D_t^{\alpha(t)} I_H = {}_0^C D_t^{\alpha(t)} I_E = 0$. Then, from (1), we have

$$f_j(\tilde{S}, \tilde{I}, \tilde{I_D}, \tilde{I_A}, \tilde{I_T}, \tilde{I_R}, \tilde{I_T}, \tilde{I_H}, \tilde{I_E}) = 0, \quad j = 1, \ldots, 8,$$

where, $(\tilde{S}, \tilde{I}, \tilde{I_D}, \tilde{I_A}, \tilde{I_T}, \tilde{I_R}, \tilde{I_T}, \tilde{I_H}, \tilde{I_E})$ denotes any equilibrium point.

Disease-free equilibrium

If $I = I_D = I_A = I_R = I_T = 0$, and the right-hand side of the system (4)–(11) are both equal to zero, we get the disease-free point as follows:

$$E_o(S, I, I_D, I_A, I_R, I_T, I_H, I_E) = (1, 0, 0, 0, 0, 0, 0, 0).$$

Endemic equilibrium

If the infected variables I, I_D, I_A, I_R, I_T are not zero, the subsystem (6)–(10) has an endemic equilibrium, [19]. If the right-hand side of the subsystem (6)– (11) is equal to zero, then the endemic equilibrium point $E^* = (\tilde{S}, \tilde{I}, \tilde{I_D}, \tilde{I_A}, \tilde{I_R}, \tilde{I_T}, \tilde{I_H}, \tilde{I_E})$ is given as follows:

From Eq. (6),

$$\tilde{S} = \frac{r_1 \tilde{I}}{\beta^{\alpha(t)} \tilde{I} + \beta_D^{\alpha(t)} \tilde{I_D} + \gamma^{\alpha(t)} \tilde{I_A} + \delta^{\alpha(t)} \tilde{I_R}}, \tag{12}$$

from equations (7)–(9), we have

$$\tilde{I_D} = \frac{\varepsilon^{\alpha(t)} \tilde{I}}{r_2}, \quad \tilde{I_A} = \frac{\zeta^{\alpha(t)} \tilde{I}}{r_3}, \tag{13}$$

$$\tilde{I_R} = \left(\frac{\eta^{\alpha(t)} \varepsilon^{\alpha(t)}}{r_2 r_4} + \frac{\zeta^{\alpha(t)} \varepsilon_A^{\alpha(t)} \tilde{I}}{r_3 r_4}\right) \tilde{I}. \tag{14}$$

By substitution in (12)

$$\tilde{S} = \frac{r_1 r_2 r_3 r_4}{\beta^{\alpha(t)} r_2 r_3 r_4 + \beta_D^{\alpha(t)} \varepsilon^{\alpha(t)} r_3 r_4 + \gamma^{\alpha(t)} \zeta^{\alpha(t)} r_2 r_4 + \delta^{\alpha(t)} (\eta^{\alpha(t)} \varepsilon^{\alpha(t)} r_3 + \zeta^{\alpha(t)} \varepsilon_A^{\alpha(t)} r_2)} \tag{15}$$

$$= \frac{1}{R_o}. \tag{16}$$

From Eq. (10)

$$\tilde{I_T} = \frac{\mu^{\alpha(t)} \tilde{I_A} + \nu^{\alpha(t)} \tilde{I_R}}{r_5}, \tag{17}$$

and $\tilde{I_H} + \tilde{I_E} = 1 - \tilde{S} - \tilde{I_D} - \tilde{I_A} - \tilde{I_R}$.

Formulation of the control problem

We will extend the necessary conditions of Pontryagin's maximum principle to variable-order fractional differentiation equations. The COVID-19 infection can be controlled and minimized in a community by maximizing the number of healed people and minimizing the number infected individuals. For this purpose, we use three suitable control variables depending on time $u_1(t)$ for the reduction of diagnosed asymptomatic infected; $u_2(t)$ for the reduction of developing life-threatening symptoms and $u_3(t)$ for the percentage of threatened population being extinct. Let,

$$J(u_1, u_2, u_3) = min \int_0^{t_f} \left(C_1 I_R(t) + C_2 I_T(t) + \frac{w_1}{2} u_1^2(t) + \frac{w_2}{2} u_2^2(t) + \frac{w_3}{2} u_3^2(t) \right) dt, \tag{18}$$

be the cost (objective) functional which will be minimize and C_1 and C_2 are the weighting constants of recognized symptomatic infected and threatened acutely symptomatic infected individuals respectively, whereas w_1, w_2 and w_3 are the positive weight constants used for the treatment of diagnosed asymptomatic infected, recognized symptomatic infected and threatened acutely symptomatic infected individuals, respectively. subjected to the constraint (4)–(11) as follows:

$$\begin{aligned}
&{}_0^C D_t^{\alpha(t)} S = -S(\beta^{\alpha(t)} I + \beta_D^{\alpha(t)} I_D + \gamma^{\alpha(t)} I_A + \delta^{\alpha(t)} I_R), \\
&{}_0^C D_t^{\alpha(t)} I = S(\beta^{\alpha(t)} I + \beta_D^{\alpha(t)} I_D + \gamma^{\alpha(t)} I_A + \delta^{\alpha(t)} I_R) - (\varepsilon^{\alpha(t)} + \zeta^{\alpha(t)} + \rho_I^{\alpha(t)}) I, \\
&{}_0^C D_t^{\alpha(t)} I_D = \varepsilon^{\alpha(t)} I - (\eta^{\alpha(t)} u_1 + \rho_D^{\alpha(t)}) I_D, \\
&{}_0^C D_t^{\alpha(t)} I_A = \zeta^{\alpha(t)} I - (\varepsilon_A^{\alpha(t)} + \mu^{\alpha(t)} + \kappa^{\alpha(t)}) I_A, \\
&{}_0^C D_t^{\alpha(t)} I_R = \eta^{\alpha(t)} u_1 I_D + \varepsilon_A^{\alpha(t)} I_A - (\nu^{\alpha(t)} u_2 + \xi^{\alpha(t)}) I_R, \\
&{}_0^C D_t^{\alpha(t)} I_T = \mu^{\alpha(t)} I_A + \nu^{\alpha(t)} u_2 I_R - (\sigma^{\alpha(t)} + d^{\alpha(t)} u_3) I_T, \\
&{}_0^C D_t^{\alpha(t)} I_H = \rho_I^{\alpha(t)} I + \rho_D^{\alpha(t)} I_D + \kappa^{\alpha(t)} I_A + \xi^{\alpha(t)} I_R + \sigma^{\alpha(t)} I_T, \\
&{}_0^C D_t^{\alpha(t)} I_E = d^{\alpha(t)} u_3 I_T,
\end{aligned} \tag{19}$$

and satisfying the initial conditions:

$$S(0) \geq 0, \; I(0) = 0, \; I_D(0) = 0, \; I_A(0) = 0, \; I_R(0) = 0,$$

$I_T(0) = 0,\ I_H(0) \geq 0,\ I_E(0) \geq 0.$

The Hamiltonian is given as following:

$$H = C_1 I_R(t) + C_2 I_T + \frac{w_1}{2}u_1^2 + \frac{w_2}{2}u_2^2 + \frac{w_3}{2}u_3^2 + \sum_{i=0}^{8} \lambda_i F_i, \tag{20}$$

where λ_i is the co-state variables $i = 1, \ldots, 8$ and F_i right hand side of system (19). From (18) and (20), we can derive the necessary conditions as follows:

$${}_{t_f}^{C} D_0^{\alpha(t)} \lambda_i(t) = \frac{\partial H}{\partial V_i},\ V_i = S,\ I,\ I_D,\ I_A,\ I_R,\ I_T,\ I_H,\ I_E, \tag{21}$$

$$\frac{\partial H}{\partial u_j} = 0,\ j = 1, 2, 3, \tag{22}$$

$$\begin{aligned}
&{}_0^{C} D_t^{\alpha(t)} S(t) = \frac{\partial H}{\partial \lambda_S},\ {}_0^{C} D_t^{\alpha(t)} I(t) = \frac{\partial H}{\partial \lambda_I},\\
&{}_0^{C} D_t^{\alpha(t)} I_D(t) = \frac{\partial H}{\partial \lambda_D},\ {}_0^{C} D_t^{\alpha(t)} I_A(t) = \frac{\partial H}{\partial \lambda_A},\\
&{}_0^{C} D_t^{\alpha(t)} I_R(t) = \frac{\partial H}{\partial \lambda_R},\ {}_0^{C} D_t^{\alpha(t)} I_T(t) = \frac{\partial H}{\partial \lambda_T},\\
&{}_0^{C} D_t^{\alpha(t)} I_H(t) = \frac{\partial H}{\partial \lambda_H},\ {}_0^{C} D_t^{\alpha(t)} I_E(t) = \frac{\partial H}{\partial \lambda_E},
\end{aligned} \tag{23}$$

and it is also required that: $\lambda_i(t_f) = 0$, where $i = S, I, I_D, A, R, T, I_H, I_E$,; are the Lagrange multipliers. Eqs. (22) and (23) describe the necessary conditions in terms of a Hamiltonian for the optimal control problem defined above.

Theorem 1. *If u_1, u_2 and u_3 are optimal controls with corresponding state $S^*, I^*, I_D^*, I_A^*, I_R^*, I_T^*, I_H^*, I_E^*$; then there are adjoint variables λ_i^*, $i = S, I, I_D, A, R, T, I_H, I_E$, :*

Case(a): *Co-state (Adjoint) equations*

$$\begin{aligned}
{}_{t_f}^{C} D_0^{\alpha(t)} \lambda_S^*(t) &= -\lambda_S^*(\beta^{\alpha(t)} I^* + \beta_D^{\alpha(t)} I_D^* + \gamma^{\alpha(t)} I_A^* + \delta^{\alpha(t)} I_R^*) + \lambda_I^*(\beta^{\alpha(t)} I^*\\
&\quad + \beta_D^{\alpha(t)} I_D^* + \gamma^{\alpha(t)} I_A^*\\
&\quad + \delta^{\alpha(t)} I_R^*),\\
{}_{t_f}^{C} D_0^{\alpha(t)} \lambda_I^*(t) &= -\lambda_S^* \beta^{\alpha(t)} S^* - \lambda_I^*(\varepsilon^{\alpha(t)} + \zeta^{\alpha(t)} + \rho_I^{\alpha(t)} - \beta^{\alpha(t)} S^*) + \lambda_A^* \zeta^{\alpha(t)} + \lambda_H^* \rho_I^{\alpha(t)},\\
{}_{t_f}^{C} D_0^{\alpha(t)} \lambda_D^*(t) &= -\lambda_S^* \beta_D^{\alpha(t)} S^* + \lambda_I^* \beta^{\alpha(t)} S^* - \lambda_D^*(\eta^{\alpha(t)} u_1^*(t) + \rho_D^{\alpha(t)})\\
&\quad + \lambda_R^* \eta^{\alpha(t)} u_1^*(t) + \lambda_H^* \rho_D^{\alpha(t)},\\
{}_{t_f}^{C} D_0^{\alpha(t)} \lambda_A^*(t) &= -\lambda_S^* \gamma^{\alpha(t)} S^* + \lambda_I^* \gamma^{\alpha(t)} S^* - \lambda_A^*(\varepsilon_A^{\alpha(t)} + \mu^{\alpha(t)} + \kappa^{\alpha(t)})\\
&\quad + \lambda_R^* \varepsilon_A^{\alpha(t)} + \lambda_T^* \mu^{\alpha(t)} + \lambda_H^* \kappa^{\alpha(t)},\\
{}_{t_f}^{C} D_0^{\alpha(t)} \lambda_R^*(t) &= C_1 - \lambda_S^* \delta^{\alpha(t)} S^* + \lambda_I^* \delta^{\alpha(t)} S^* - \lambda_R^*(\nu^{\alpha(t)} u_2^*(t) + \xi^{\alpha(t)})\\
&\quad + \lambda_T^* \nu^{\alpha(t)} u_2^*(t) + \lambda_H^* \xi^{\alpha(t)},\\
{}_{t_f}^{C} D_0^{\alpha(t)} \lambda_T^*(t) &= C_2 - \lambda_T^*(\sigma^{\alpha(t)} u_3^*(t) + d^{\alpha(t)}) + \lambda_H^* \sigma^{\alpha(t)} + \lambda_T^* d^{\alpha(t)} u_3(t),\\
{}_{t_f}^{C} D_0^{\alpha(t)} \lambda_H^*(t) &= 0,\\
{}_{t_f}^{C} D_0^{\alpha(t)} \lambda_E^*(t) &= 0.
\end{aligned} \tag{24}$$

Case(b): *The transversality conditions:*

$$\lambda_i^*(t_f) = 0,\ \ i = S, I, I_D, A, R, T, I_H, I_E.$$

Case(c): *optimality conditions:*
From (22), the control functions u_1^*, u_2^* and u_3^*:

$$u_1^* = min\{1, max\{0, \frac{\eta^{\alpha(t)} I_D(\lambda_D - \lambda_H)}{w_1}\}\},$$

$$u_2^* = min\{1, max\{0, \frac{\nu^{\alpha(t)} I_R(\lambda_R - \lambda_H)}{w_2}\}\}$$

and

$$u_3^* = min\{1, max\{0, \frac{d^{\alpha(t)} I_T(\lambda_T - \lambda_H)}{w_2}\}\}.$$

Now, by substituting u_1^*, u_2^* and u_2^* in (19), we have the state equations as follows:

$$\begin{aligned}
&{}_0^{C} D_t^{\alpha(t)} S^* = -S^*(\beta^{\alpha(t)} I^* + \beta_D^{\alpha(t)} I_D^* + \gamma^{\alpha(t)} I_A^* + \delta^{\alpha(t)} I_R^*),\\
&{}_0^{C} D_t^{\alpha(t)} I^* = S^*(\beta^{\alpha(t)} I^* + \beta_D^{\alpha(t)} I_D^* + \gamma^{\alpha(t)} I_A^* + \delta^{\alpha(t)} I_R^*) - (\varepsilon^{\alpha(t)} + \zeta^{\alpha(t)} + \rho_I^{\alpha(t)}) I^*,\\
&{}_0^{C} D_t^{\alpha(t)} I_D^* = \varepsilon^{\alpha(t)} I^* - (\eta^{\alpha(t)} u_1^* + \rho_D^{\alpha(t)}) I_D^*,\\
&{}_0^{C} D_t^{\alpha(t)} I_A^* = \zeta^{\alpha(t)} I^* - (\varepsilon_A^{\alpha(t)} + \mu^{\alpha(t)} + \kappa^{\alpha(t)}) I_A^*,\\
&{}_0^{C} D_t^{\alpha(t)} I_R^* = \eta^{\alpha(t)} u_1^* I_D^* + \varepsilon_A^{\alpha(t)} I_A^* - (\nu^{\alpha(t)} u_2^* + \xi^{\alpha(t)}) I_R^*,\\
&{}_0^{C} D_t^{\alpha(t)} I_T^* = \mu^{\alpha(t)} I_A^* + \nu^{\alpha(t)} u_2^* I_R^* - (\sigma^{\alpha(t)} + d^{\alpha(t)} u_3^*) I_T^*,\\
&{}_0^{C} D_t^{\alpha(t)} I_H = \rho_I^{\alpha(t)} I + \rho_D^{\alpha(t)} I_D + \kappa^{\alpha(t)} I_A + \xi^{\alpha(t)} I_R^* + \sigma^{\alpha(t)} I_T^*,\\
&{}_0^{C} D_t^{\alpha(t)} I_E^* = d^{\alpha(t)} u_3^* I_T^*,
\end{aligned} \tag{25}$$

Numerical methods

The mathematical models (25) and (24) will be studied in this section, moreover, two non-standard methods are constructed in the next sections.

A numerical method is considered non-standard if at least one of the following conditions is satisfied [21]:

1-It is decided to use the non-local approximation.

2- Discretization of a derivative is not traditional and use a nonnegative function,

$$\varphi(h) = h + O(h^2),\ \ 0 < \varphi < 1,\ \ \forall\ h > 0,$$

We will give a quick rundown of these methods:

NGRK4M

Let a collection of mesh points $\Im = \{t_0, t_1, \ldots, t_n\}$, such that $t_0 = 0$, $t_n = T$, T is the final time and $h = \frac{T}{n}$, $n = 1, 2, \ldots, N$.

Now, we can write the approximation solution of Eq. (1) [22]:

$$y_{n+1} = \frac{1}{6}(K_1 + 2K_2 + 2K_3 + K_4) + y_n, \tag{26}$$

$$K_1 = \kappa f(t_n, y_n),$$

$$K_2 = \kappa f(t_n + \frac{1}{2}\kappa, y_n + \frac{1}{2}K_1),$$

$$K_3 = \kappa f(t_n + \frac{1}{2}\kappa, y_n + \frac{1}{2}K_2),$$

$$K_4 = \kappa f(t_n + \kappa, y_n + K_3), \qquad \kappa = (\Gamma(\alpha(t) + 1))^{-1} \varphi(h)^{\alpha(t)}.$$

For more details on the fractional NGRK4M stability analysis, see [10]. We use the proposed method to solve (25) with initial condition. Also, we discretize (24) with transitivity condition using the same technique with backward in time discretization, we get system of algebraic equations which can be solved easily.

NGRK5M

Let a collection of mesh points $\Im = \{t_0, t_1, \ldots, t_n\}$, such that $t_0 = 0$, and $t_n = T$, $h = \frac{T}{n}$, $n = 1, 2, \ldots, N$.

In the proposed GRK5M [22], to approximate solution for Eq. (1), we will substitute the step size in GRK5M, by a function in h, and this function is continuous:

The general formula for NGRK5M type 1 is given as follows:

$$y_{n+1} = y_n + \frac{1}{90}(7K_1 + 32K_3 + 12K_4 + 32K_5 + 7K_6), \tag{27}$$

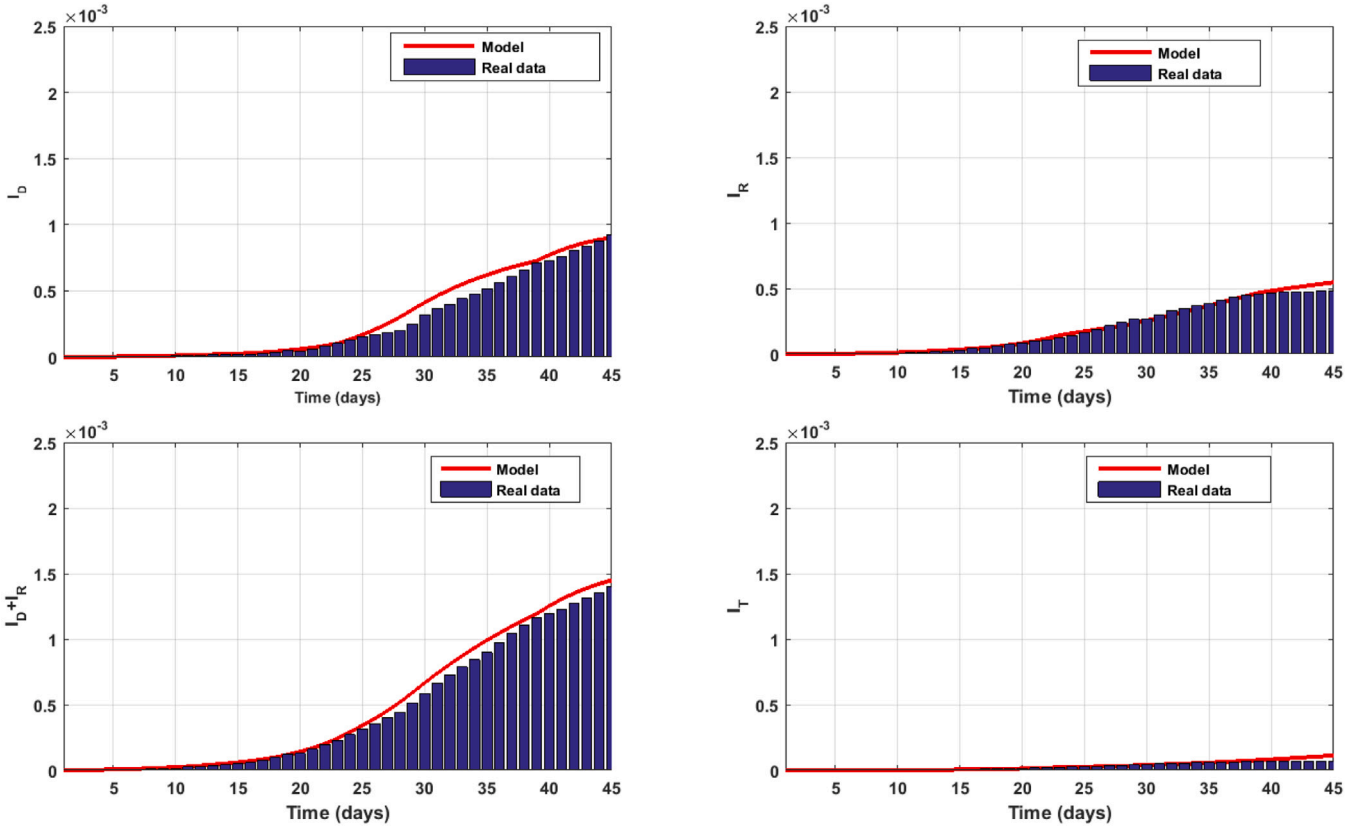

Fig. 1. Real data compared to the approximate solutions using GRK5M, when $\alpha(t) = 1$.

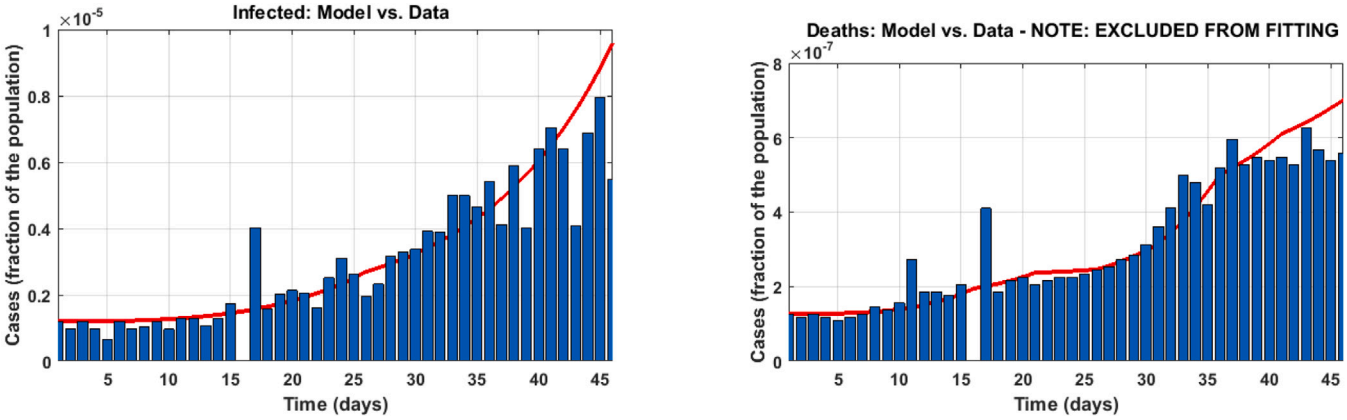

Fig. 2. Approximate solutions behavior compared to real data in Egypt, when $\alpha(t) = 1$.

$$K_1 = \kappa f(t_n, y_n),$$

$$K_2 = \kappa f(t_n + \frac{1}{4}\kappa, y_n + \frac{1}{4}K_1),$$

$$K_3 = \kappa f(t_n + \frac{1}{4}\kappa, y_n + \frac{1}{8}K_1 + \frac{1}{8}K_2),$$

$$K_4 = \kappa f(t_n + \frac{1}{2}\kappa, y_n - \frac{1}{2}K_2 + K_3),$$

$$K_5 = \kappa f(t_n + \frac{3}{4}\kappa, y_n + \frac{3}{16}K_1 + \frac{9}{16}K_4),$$

$$K_6 = \kappa f(t_n + \kappa, y_n - \frac{3}{7}K_1 + \frac{2}{7}K_2 + \frac{12}{7}K_3 - \frac{12}{7}K_4 + \frac{8}{7}K_5), \quad \kappa = \frac{\varphi(h)^{\alpha(t)}}{\Gamma(\alpha(t)+1)}.$$

We use the proposed method to solve (25) with initial condition. Also, we discretize (24) with transitivity condition using the same technique with backward in time discretization, we get system of algebraic equations which can be solved easily.

- **Stability analysis of NGRK5M type 1**

To study the stability of NSRK5M. Consider (1), then, we can approximate (1) using NGRK5M type 1 as:

$$y(t_{j+1}) = y(t_j) + \frac{1}{\varphi(h)^{-\alpha(t)}(1+\Gamma(\alpha(t)))90} G(t_j, y(t_j)) + O(\varphi(h)^{5\alpha(t_j)}), \quad (28)$$

$j = 0, 1, \ldots, n-1.$

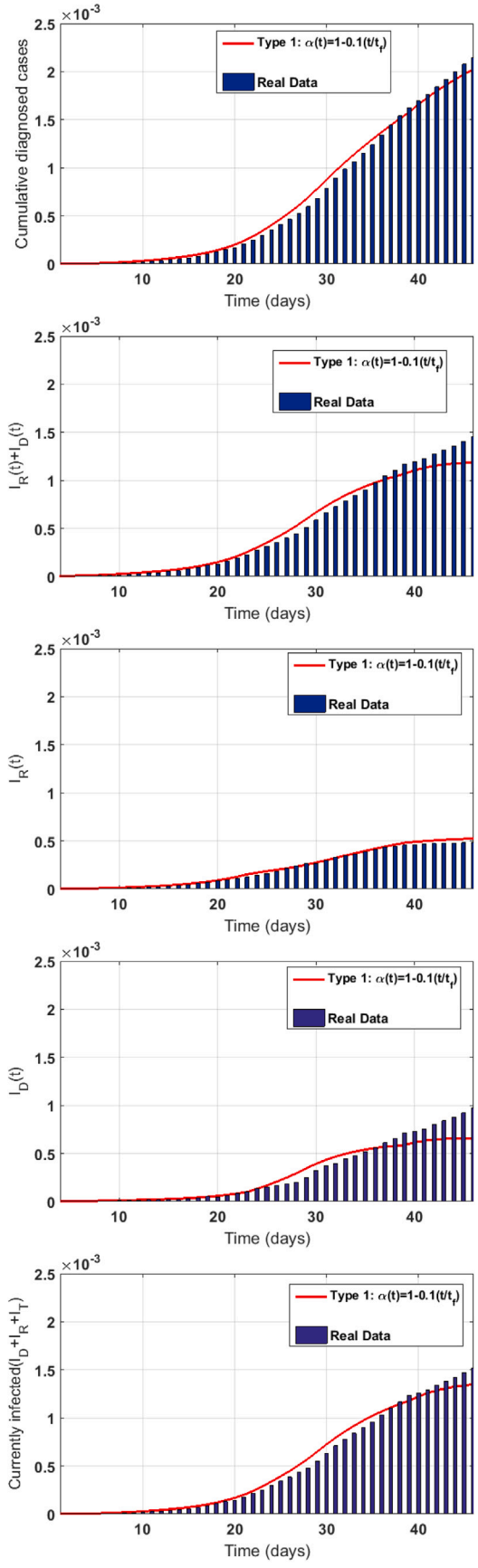

Fig. 3. Behavior of the approximate solutions compared to real data, when $\alpha(t) = 1 - 0.1(t/t_f)$ type one using GRK5M.

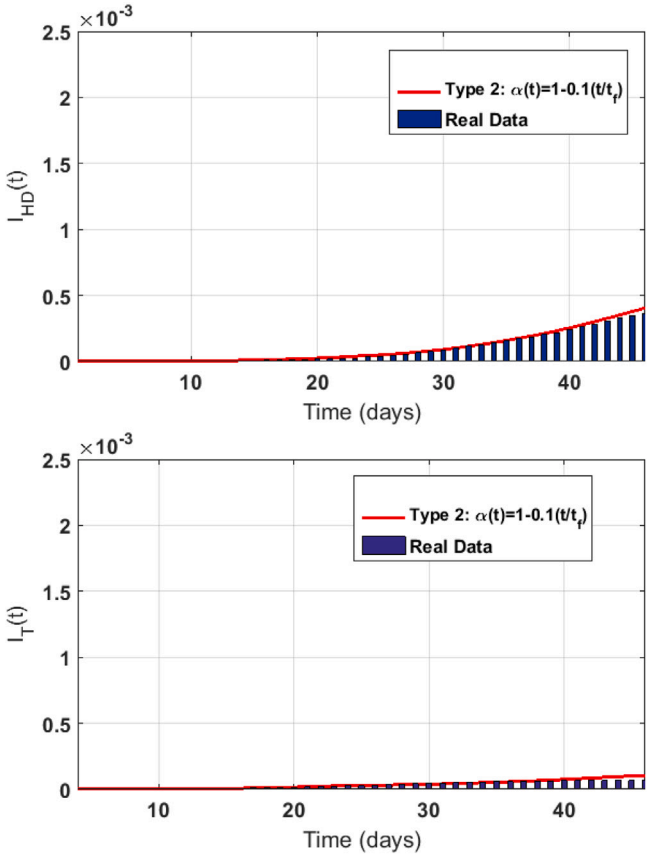

Fig. 4. Behavior of the approximate solutions compared to real data, when $\alpha(t) = 1 - 0.1(t/t_f)$ type two using GRK5M.

In order to study the stability of proposed method (28), the test problem is used as follows:

$$ {}_0^C D_t^{\alpha(t)} y(t) = \upsilon y(t), \quad \upsilon < 0, \quad T > t \geq 0, \quad 1 > \alpha(t) \geq 0, \tag{29} $$

$$ y(0) = y_0. $$

The solution is asymptotically stable if υ is a negative number and becomes unstable if υ is positive and increasing, [9]. NGRK5M is applied to (29), the equation becomes:

$$ y(t_{j+1}) = y(t_j) + \frac{1}{90} \frac{\varphi(h)^{\alpha(t)} \upsilon}{\Gamma(1+\alpha(t))} y(t_j), \quad j = 0, 1, \ldots, n-1, \tag{30} $$

$$ = (1 + \frac{1}{90} \frac{\varphi(h)^{\alpha(t)} \upsilon}{\Gamma(\alpha(t)+1)})^j y_0. \tag{31} $$

Therefore the stability condition:

$$ \left| (1 + \frac{\upsilon}{90} \frac{1}{\varphi(h)^{-\alpha(t)} \Gamma(1+\alpha(t))}) \right| < 1. $$

The general formula for NGRK5M type 2 is given as follows:

$$ y_{n+1} = y_n + \frac{1}{90}(7K_1 + 32K_3 + 12K_4 + 32K_5 + 7K_6), \tag{32} $$

$$ K_1 = \kappa f(t_n, y_n), $$

$$ K_2 = \kappa f(t_n + \frac{1}{4}\kappa, y_n + \frac{1}{4}K_1), $$

$$ K_3 = \kappa f(t_n + \frac{1}{4}\kappa, y_n + \frac{1}{8}K_1 + \frac{1}{8}K_2), $$

$$ K_4 = \kappa f(t_n + \frac{1}{2}\kappa, y_n - \frac{1}{2}K_2 + K_3), $$

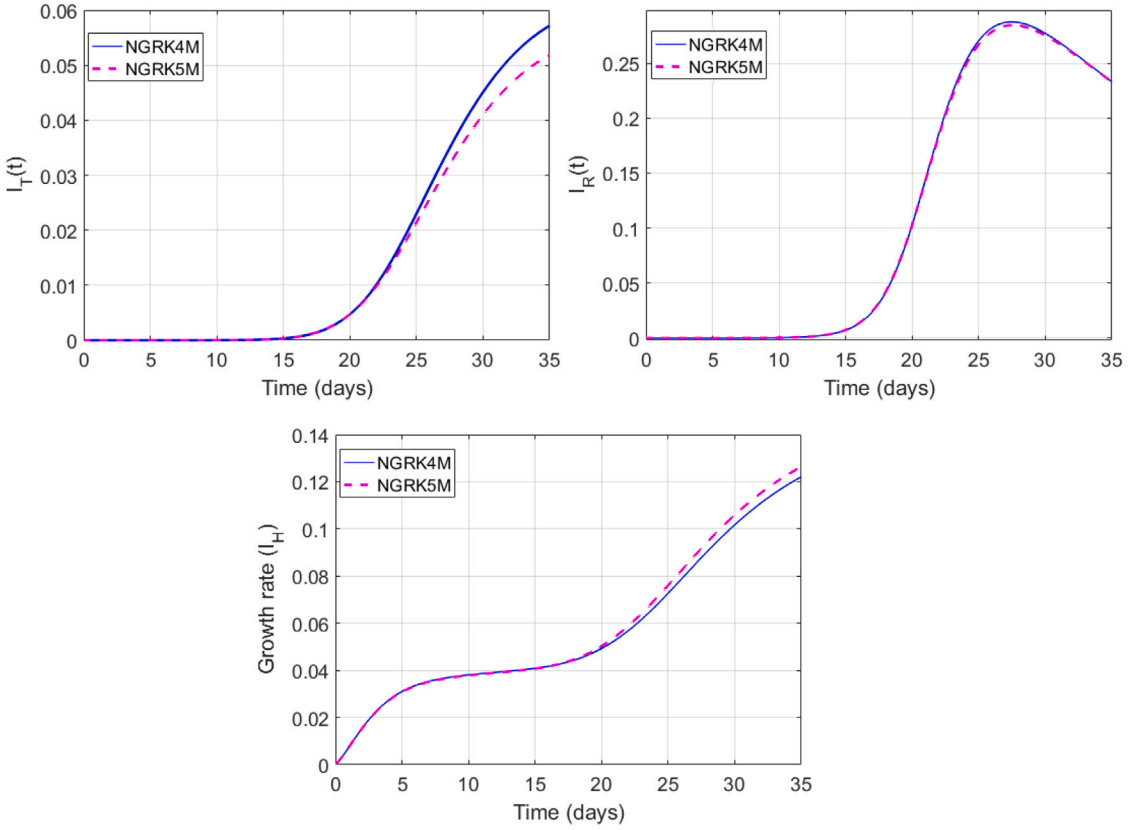

Fig. 5. Behavior of the approximate solutions of I_R, I_T and the growth rate of I_H at different methods when $\alpha(t) = 1 - 0.004(t/t_f)$.

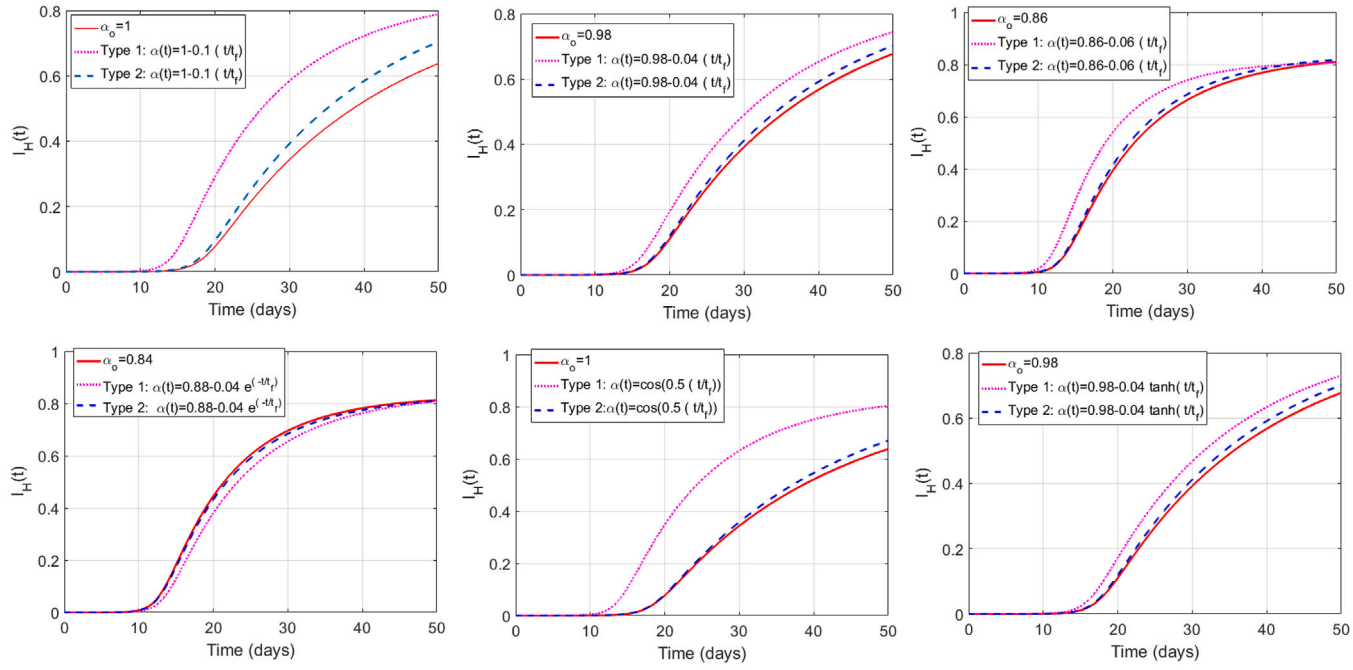

Fig. 6. Optimization of the approximation solutions of I_H at different types of $\alpha(t)$.

$$K_5 = \kappa f(t_n + \frac{3}{4}\kappa, y_n + \frac{3}{16}K_1 + \frac{9}{16}K_4),$$

$$K_6 = \kappa f(t_n + \kappa, y_n - \frac{3}{7}K_1 + \frac{2}{7}K_2 + \frac{12}{7}K_3 - \frac{12}{7}K_4 + \frac{8}{7}K_5),$$

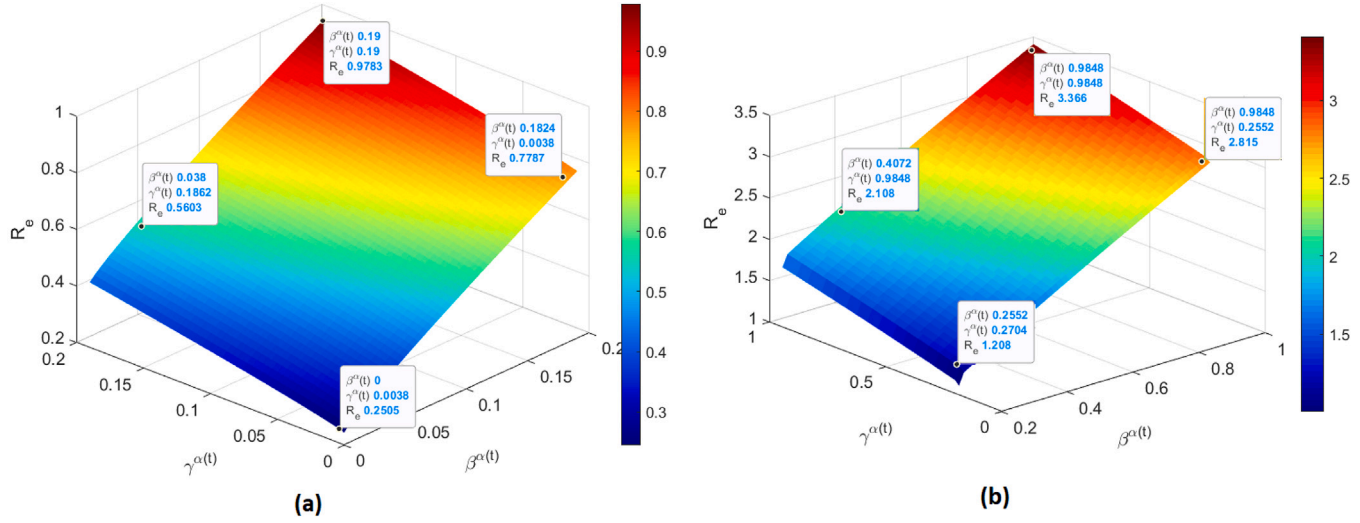

Fig. 7. The impact of $\beta^{\alpha}(t)$ and $\gamma^{\alpha}(t)$ on behavior of R_e at $\alpha(t) = 0.9 - 0.2(t/t_f)$. Case(a) when $R_e < 1$ and case (b) when $R_e > 1$.

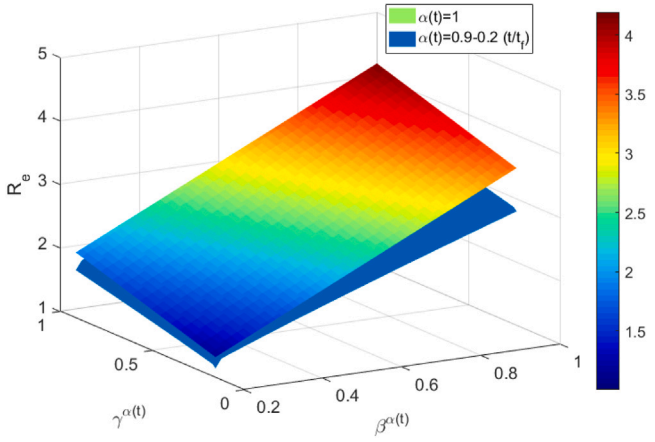

Fig. 8. The impact of $\beta^{\alpha}(t)$ and $\gamma^{\alpha}(t)$ on behavior of R_e at different value of $\alpha(t)$.

and $\frac{\varphi(h)^{\alpha(t_n)}}{\Gamma(\alpha(t_n)+1)} = \kappa$. We use the proposed method to solve (25) with initial condition. Also, we discretize (24) with transitivity condition using the same technique with backward in time discretization, we get system of algebraic equations which can be solved easily.

- **Stability of NGRK5M type 2**

In the following, we can approximate (1) using NGRK5M type 2 as:

$$y(t_{j+1}) = y(t_j) + \frac{1}{\varphi(h)^{-\alpha(t_j)}(\Gamma(1+\alpha(t_j)))90} G(t_j, y(t_j)) + O(\varphi(h)^{5\alpha(t_j)}), \quad (33)$$

$j = 0, 1, \ldots, n-1.$

Using (29) and (32), we have:

$$y(t_{j+1}) = y(t_j) + \frac{1}{90}\frac{\upsilon}{\varphi(h)^{-\alpha(t_j)}\Gamma(1+\alpha(t_j))} y(t_j), \quad j = 0, 1, \ldots, n-1, \quad (34)$$

$$= (1 + \frac{1}{90}\frac{\upsilon}{\varphi(h)^{-\alpha(t_j)}\Gamma(1+\alpha(t_j))})^j y_0. \quad (35)$$

Therefore, the stability condition:

$$\left|(1 + \frac{\upsilon}{90}\frac{\varphi(h)^{\alpha(t_j)}}{\Gamma(\alpha(t_j)+1)})\right| < 1.$$

The algorithm of NGRK5M

This algorithm consists of the following steps:

Consider $\tilde{x} = (x_1; \ldots; x_{N+1})$ and $\tilde{\lambda} = (\lambda_1; \ldots; \lambda_{N+1})$ represent the vector approximations for the state and adjoint systems respectively.

Step 1. Make an initial guess for $\tilde{u_1}, \tilde{u_2}$ and $\tilde{u_3}$.

Step 2. Solve $\tilde{x}$ forward NGRK5M in time, using the initial condition $x_1 = x(t_0)$ and the values for $\tilde{u_1}, \tilde{u_2}$ and $\tilde{u_3}$.

Step 3. Solve $\tilde{\lambda_i}$ backward NGRK5M in time using the transversality condition $\tilde{\lambda}_{N+1} = \lambda(t_1) = 0$ and the values for $\tilde{u_1}, \tilde{u_2}$ and $\tilde{u_3}$ and $\tilde{x}$.

Step 4. By entering the new $\tilde{x}$ and $\tilde{\lambda}$ values into the characterization of the optimal control, update $\tilde{u_1}, \tilde{u_2}$ and $\tilde{u_3}$.

Step 5. Output the current values as solutions, if values of the variables in this iteration and the last iteration are negligibly close. Return to Step 2, if values are not close.

Numerical simulations

The solutions of the variable-order fractional optimality systems (24) and (25) are simulated using two numerical methods in this section. These methods are NGRK4M and NGRK5M forward with time to solve the state system (25) with initial condition and backward with time to solve the co-state systems (24) with transversality conditions:

$$\lambda_i^*(t_f) = 0, \quad i = S, I, I_D, A, R, T, I_H, I_E.$$

. Also, we will use the modified parameters from Table 2. We consider the initial states of the population at day is set as [2]: $I(1) = 200/60e6$, $I_D(1) = 20/60e6$, $I_A(1) = 1/60e6$, $I_R(1) = 2/60e6$, $I_T(0) = 10$, $I_H = 0$, $I_E(1) = 0$, and $S(1) = 1 - I(1) - I_D(1) - I_A(1) - I_R(1) - I_T(1) - I_H(1) - I_E(1)$, where Italian population (60 *million*) and Egyptian population (100500159). Figs. 1–4, show the comparison between the behavior of approximation solutions and real data [2], using GRK5M and different $\alpha(t)$. The number of diagnosed recovered cases represent as:

$$I_{HD} = \int_0^t (\rho_D^{\alpha(t)} I_D(\phi) + \xi^{\alpha(t)} I_R(\phi)) + \sigma^{\alpha(t)} I_T(\phi) d\phi.$$

Also, the number of cumulative diagnosed cases are the sum of the following variables I_D, I_R, I_T, I_E, I_{HD}.

Table 3, shows the values of the objective functional for different $\alpha(t)$ with and without controls using NGRK5M when $\varphi(h) = 0.2(1-e^{-5h})$. Fig. 5, shows the behavior of the solutions the threatened population I_T, the recognized population I_R and the growth rate of recovered population $I_H(t)$ using different methods in case $\alpha(t) = -0.004(t/t_f) + 1$

Table 3
The values of objective functional J and $t \in [0, 100]$ using NGRK5M.

$\alpha(t)$	J values without controls	J values with controls
$\alpha(t) = 1$	20.3132	10.4946
$\alpha(t) = 1 - 0.009t$	17.5503	9.6116
$\alpha(t) = 1 - 0.001(cos^2(t))$	20.3113	10.4971
$\alpha(t) = 1 - 0.05cos(10t)$	19.4945	10.4954
$\alpha(t) = 0.98$	20.0478	10.4552
$\alpha(t) = 0.98 - 0.001t$	15.4357	8.7975
$\alpha(t) = 0.85 - 0.0001t$	10.582	6.6575
$\alpha(t) = 0.99 - 0.001sin(t)$	20.2403	10.4981
$\alpha(t) = 0.90 - 0.001sin^2(t)$	15.3228	8.7522
$\alpha(t) = 0.95 - 0.05cos^2(t)$	18.5981	9.9883

and $\varphi(h) = 2(-e^{-h} + 1)$. We noted that the results obtained by NGRK5M are better than the result obtained by NGRK4M. Fig. 6, illustrates the solution for I_H using NGRK5M with linear and nonlinear $\alpha(t)$ when $\varphi(h) = 2(1 - e^{-h})$ and at three different cases of $\alpha(t)$ i.e., $\alpha(t)$ is constant order and $\alpha(t)$ is defined using type 1 of NGRK5M and type 2 of NGRK5M. We noted that the results obtained by type 2 of NGRK5M are convergent to the solution obtained by constant fractional order better than the results obtained by type 1 of NGRK5M. Figs. 7 and 8 show the impact of $\beta^{\alpha(t)}$ and $\gamma^{\alpha(t)}$ on behavior of R_e at different values of $\alpha(t)$. We noted that the model of variable-order is general model than the model of fractional order and integer order, new behavior of the solution is appeared by using different values of $\alpha(t)$.

Conclusions

The current paper analyzed a novel optimal control variable-order COVID-19 pandemic with modified parameters. Moreover, two variable order definitions in the Caputo's sense are presented to extended the COVID-19 pandemic model. From the comparison with real data from Egypt and Italy, we concluded that the proposed model is described well the real data in Italy compared the real data in Egypt. Specifically, we had successfully applied a kind of Pontryagin's maximum principle to reduce the threatened population by using three suitable control variables depending on time. NGRK4M and NGRK5M are constructed to solve the optimality system. We can claim from Fig. 6 that the solutions obtained using CVOT2 is the best. Numerical outcomes are introduced to show the validity and applicability of the proposed scheme. In future, the present study can be extended to piecewise differential model.

CRediT authorship contribution statement

Nasser Sweilam: Conceptualization, Data curation, Formal analysis, Funding acquisition, Resources, Methodology, Investigation, Supervision, Writing – review & editing. **Seham Al-Mekhlafi:** Conceptualization, Data curation, Formal analysis, Funding acquisition, Resources, Software, Validation, Visualization, Writing – original draft, Methodology, Investigation, Supervision. **Salma Shatta:** Software, Validation, Visualization, Writing – original draft. **Dumitru Baleanu:** Supervision, Writing – review & editing.

Declaration of competing interest

The authors declare that they have no known competing financial interests or personal relationships that could have appeared to influence the work reported in this paper.

Data availability

No data was used for the research described in the article.

Acknowledgments

The authors are grateful to all anonymous reviewers for their valuable comments which have provided great help for the improvement of the paper.

Funding

This research received no specific grant from any funding agency in the public, commercial, or not-for-profit sectors.

References

[1] World Health Organization. Coronavirus. World HealthOrganization; 2020, cited January 19, 2020. Available: https://www.who.int/health-topics/coronavirus.
[2] Giordano G, Blanchini F, Bruno R, Colaneri P, Di Filippo A, Di Matteo A, Colaneri M. Modelling the COVID-19 epidemic and implementation of population-wide interventions in Italy. Nat Med https://doi.org/10.1038/s41591-020-0883-7.
[3] Kumar S, Kumar R, Osman MS, Samet B. A wavelet based numerical scheme for fractional order SEIR epidemic of measles by using Genocchi polynomials. Numer Methods Partial Differential Equations 2021;37:1250–68. http://dx.doi.org/10.1002/num.2257.
[4] Mohammadi H, Kumar S, Rezapour S, Etemad S. A theoretical study of the Caputo–Fabrizio fractional modeling for hearing loss due to Mumps virus with optimal control. Chaos Solitons Fractals 2021;144:110668.
[5] Solís-Pérez JE, Gómez-Aguilar JF. Novel numerical method for solving variable-order fractional differential equations with power, exponential and Mittag-Leffler laws. Chaos Solitons Fractals 2018;14:175–85.
[6] Sun H, Chang A, Zhang Y, Chen W. A review on variable-order fractional differential equations: mathematical foundations, physical models, and its applications. Fract Calc Appl Anal 2019;22(1):27–59.
[7] Sweilam NH, AL-Mekhlafi SM. Numerical study for multi-strain tuberculosis(TB) model of variable-order fractional derivatives. J Adv Res 2016;7(2):271–83.
[8] Sweilam NH, Al-Mekhlafi SM, Albalawi AO. A novel variable-order fractional nonlinear Klein Gordon model: a numerical approach. Numer Methods Partial Differential Equations 2019;35(5):1617–29.
[9] Sweilam NH, AL-Mekhlafi SM. Optimal control for a nonlinear mathematical model of tumor under immune suppression: a numerical approach. Optimal Control Appl Methods 2018;39(5):1581–96. http://dx.doi.org/10.1002/oca.2427.
[10] Sweilam NH, AL-Mekhlafi SM, Shatta SA. Optimal bang–bang control for variable-order dengue virus; numerical studies. J Adv Res 2021. http://dx.doi.org/10.1016/j.jare.2021.03.010.
[11] Sweilam NH, AL-Mekhlafi SM, Shatta SA. On the awareness programs of the epidemic outbreaks fractional model. J Fract Calc Appl 2020;11(1):26–40. http://dx.doi.org/10.1002/oca.2427.
[12] Sweilam NH, AL-Mekhlafi SM, Shatta SA, Baleanu D. Numerical study for a novel variable-order multiple time delay awareness programs mathematical model. Appl Numer Math 2020;158:212–35.
[13] Sweilam NH, AL-Mekhlafi SM, Shatta SA, Baleanu D. Numerical study for two types variable-order Burgers' equations with proportional delay. Appl Numer Math 2020;156:364–76.
[14] Sweilam NH, AL-Mekhlafi SM, Alshomrani AS, Baleanu D. Comparative study for optimal control nonlinear variable-order fractional tumor model. Chaos Solitons Fractals 2020;136.
[15] Sweilam NH, AL Mekhlafi SM, Albalawi AO, Tenreiro Machado JA. Optimal control of variable-order fractional model for delay cancer treatments. Appl Math Model 2020;89:1557–74.
[16] Sweilam NH, AL-Mekhlafi SM, Mohammed ZN, Baleanu D. Optimal control for variable order fractional HIV/AIDS and malaria mathematical models with multi-time delay. Alex Eng J 2020. http://dx.doi.org/10.1016/j.aej.2020.07.021.
[17] WHO Coronavirus Disease (COVID-19), Egypt, https://covid19.who.int/table.
[18] Sun HG, Chen W, Wei H, Chen YQ. A comparative study of constant order and variable order fractional models in characterizing memory property of systems. Eur Phys J Spec Top 2011;193:185–92.
[19] Van den Driessche P, Watmough J. Reproduction numbers and subthreshold endemic equilibria for compartmental models of disease transmission. Math Biosci 2002;180:29–48.
[20] Van den Driessche J. Watmough P. Reproduction numbers and sub-threshold endemic equilibria for compartmental models of disease transmission. Math Biosci 2002;180:29–48.
[21] Mickens RE. Nonstandard finite difference models of differential equations. Singapore: World Scientific; 2005.
[22] Milici C, Machado JT, Draganescu G. Application of the Euler and Runge–Kutta generalized methods for FDE and symbolic packages in the analysis of some fractional attractors. Int J Nonlinear Sci Numer Simul 2019;21(2).